Progress In Electromagnetics Research C, Vol. 21, 1–12, 2011

COLLISION OF NONLINEAR ENVELOPE PULSES DEVELOPED IN COMPOSITE RIGHT- AND LEFT-HANDED TRANSMISSION LINES PERIODICALLY LOADED WITH SCHOTTKY VARACTORS

K. Narahara

Graduate School of Science and Engineering
Yamagata University
4-3-16 Jonan, Yonezawa, Yamagata 992-8510, Japan

Abstract—We investigate numerically the collision of nonlinear envelope pulses in composite right- and left-handed transmission lines with regularly spaced Schottky varactors. Because of the nonlinearity caused by the Schottky varactors, the dispersive distortion of envelope pulses is well compensated. We find that when two nonlinear envelope pulses traveling in the opposite directions collide, two envelope pulses are newly developed. The carrier wave frequency of the newly developed pulse is the harmonic of the colliding pulses that satisfies the phase-matching condition.

1. INTRODUCTION

A nonlinear transmission line (NLTL) is defined as a lumped transmission line containing a series inductor and a shunt Schottky varactor in each section [1]. NLTLs are used for the development of solitons and are employed in high-speed electronic circuits such as an electrical shock generator [2]. Recently, we consider the weakly dispersive coupled NLTLs [3]. It is well-known that the c mode and π mode are two different propagation modes on a linear coupled line. We find that both modes can support soliton-like pulses, and small c-mode pulses are generated by the collision of two π-mode pulses traveling in the opposite directions. It is expected that similar properties can be observed in strongly dispersive nonlinear lines.

Received 10 March 2011, Accepted 31 March 2011, Scheduled 1 April 2011
Corresponding author: Koichi Narahara (narahara@yz.yamagata-u.ac.jp).

We consider composite right- and left-handed (CRLH) transmission lines [4]. Several interesting managements of dispersive properties of propagating waves have been investigated [5, 6]. A CRLH line also receives attention as a platform for pulse managements [7]. Wave properties in purely LH transmission lines whose series capacitors are replaced by the varactors have also been investigated [8–12]. We considered the situation where each shunt capacitor was replaced with the Schottky varactor, such that the dispersion of CRLH lines can be compensated through the nonlinearity introduced by the varactors, resulting in a soliton-like envelope pulse [13]. As expected, we found that the collision of two nonlinear envelope pulses leads to the development of a pair of envelope pulses (one travels forward and the other backward). This paper discusses the detailed properties of this newly developed envelope pulses.

We first review briefly the fundamental aspects of nonlinear pulses in the Schottky CRLH lines, including the circuit configuration, dispersive properties, and predictions given by the nonlinear Schrödinger equation that perturbatively models the line. We next discuss several results of time-domain calculations that describe the collision of two nonlinear envelope pulses to characterize the pulses newly developed by the collision. The relationship of the wave numbers and carrier frequencies between the colliding and newly developed pulses is examined to see that the phase-matching condition determines the properties of the newly developed pulses.

2. SCHOTTKY CRLH LINES

Figure 1(a) shows a unit cell of the line under investigation. The parameters L_R, C_L, and L_L are the series inductance, series capacitance, and shunt inductance, respectively. The shunt capacitance is represented by C_R. As the source of nonlinearity, the Schottky varactor is employed for C_R. Its capacitance voltage relationship is generally defined as

$$C_R(V) = \frac{C_0}{\left(1 - \frac{V}{V_J}\right)^m}, \tag{1}$$

where C_0, V_J, and m are the zero-bias junction capacitance, junction potential, and grading coefficient, respectively. Hereafter, the bias voltage of the Schottky varactor is represented by V_0, and $C_R(V_0)$ is denoted by $C_R^{(0)}$ for brevity. Using this representation, the transmission

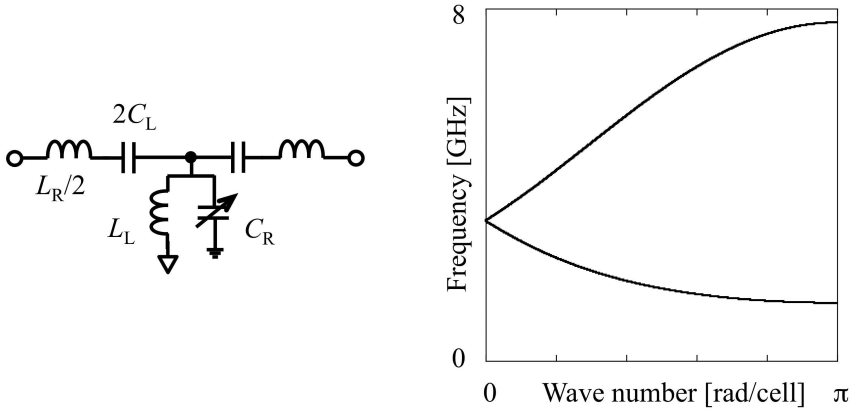

Figure 1. Schottky CRLH lines. (a) The unit cell and (b) the dispersion of the line.

equations are given by

$$L_R \frac{d^2 I_n}{dt^2} = -\frac{I_n}{C_L} - \frac{d}{dt}\left(V_n - V_{n-1}\right), \tag{2}$$

$$C_R \frac{d^2 V_n}{dt^2} = -\frac{V_n}{L_L} + \frac{d}{dt}\left(I_n - I_{n+1}\right) - \frac{dC_R}{dV_n}\left(\frac{dV_n}{dt}\right)^2, \tag{3}$$

where I_n and V_n are the current and voltage at the nth cell, respectively.

We first linearize Eqs. (2), (3) to examine the dispersive property of the line. The dispersion relationship is then shown in Fig. 1(b). We set $C_R^{(0)}$, C_L, L_R, and L_L to 1.0 pF, 1.0 pF, 2.5 nH, 2.5 nH, respectively. The line is *balanced* for this example. The wave number becomes zero at the frequency $f_0 \equiv 1/2\pi\sqrt{C_L L_R}$ (= 3.2 GHz). The line exhibits the left- (right-)handedness for frequencies less (greater) than f_0.

In order to investigate the contributions of nonlinearity, we apply the reductive perturbation method [14] to Eqs. (2) and (3). We then obtain the nonlinear Schrödinger (NS) equation whose dispersion and nonlinearity coefficients determine the properties of nonlinear envelope pulses. See Ref. [13] for the explicit expressions for the dispersion coefficient p and the nonlinearity coefficient q. The pulse width of the single soliton with the amplitude of A_0 is given by $(A_0 v_g \sqrt{q/8p})^{-1}$, where v_g represents the group velocity. In Fig. 2, we show the dependence of the pulse width of a single solition with $A_0 = 1.0\,\mathrm{V}$

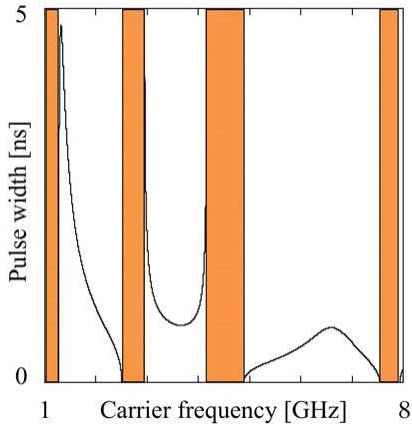

Figure 2. Pulse width of single soliton developed in Schottky CRLH lines. At the filled frequencies, the development of bright solitons is prohibited.

on the carrier frequency. For the Schottky varactor, V_0, m, and V_J are set to $-1.0\,\mathrm{V}$, 2.0, and $2.0\,\mathrm{V}$, respectively. Because $p \cdot q$ becomes negative, bright solitons cannot develop in the filled frequency range.

3. COLLISION OF TWO NONLINEAR ENVELOPE PULSES

To characterize the collision of two nonlinear envelope pulses, we numerically solved Eqs. (2), (3) for the same parameters as used to obtain Fig. 1(b) and Fig. 2. First, we solved the loss-free line. Total cell size was 4000 to ensure the time window to discriminate the colliding and newly developed pulses.

Figure 3 shows the properties for the colliding pulses with 1.6-GHz carrier frequencies. The carrier wave with the fundamental frequency ($1.6\,\mathrm{GHz}$) is located at P_1 on the dispersion curve in Fig. 3(a). Moreover, the 2nd, 3rd, and 4th harmonics correspond to P_2, P_3, and P_4, respectively. Note that the wave number of the 2nd harmonic is nearly equal to zero. On the other hand, Fig. 3(b) shows the numerically obtained waveforms. The width of the incident pulse was set to $4.1\,\mathrm{ns}$, which was given by the analytically expected value for a single bright soliton with 0.3-V amplitude. Six spatial waveforms recorded in 60-ns increments are shown. As indicated by the red circles, long-wavelength envelope pulses develop by the collision. Figs. 4(a) and (b) show the temporal waveforms of the incident and

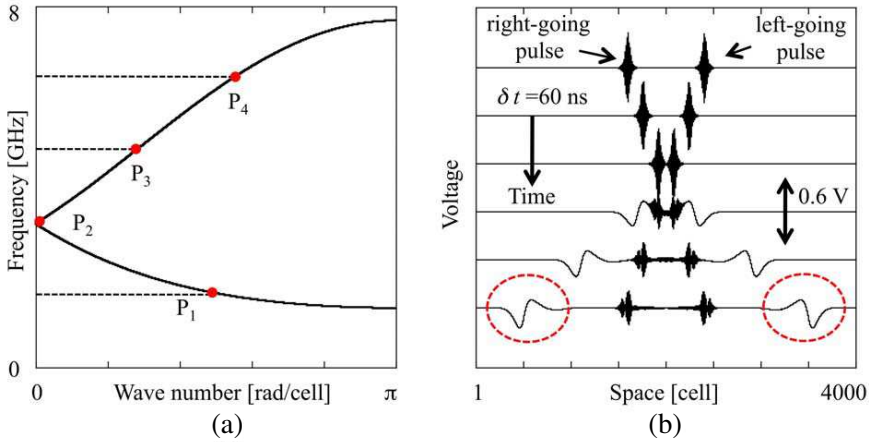

Figure 3. Collision of two nonlinear envelope pulses with 1.6-GHz carrier frequencies. The positions of the fundamental and harmonics on the dispersion curve are shown in Fig. 3(a). The fundamental, 2nd-, 3rd-, and 4th-harmonic are represented by P_1, P_2, P_3, and P_4, respectively. Six spatial waveforms recorded in 60-ns increments are shown in Fig. 3(b). The newly developed pulses are marked with the circles.

newly developed pulses monitored at the 1000th cell. We can see that both pulses have isolated shapes. The Fourier analysis proves that the newly developed pulse has the spectral peak at 3.2 GHz, i.e., the 2nd harmonic of the incident pulses.

Another example is shown in Fig. 5. At present, the carrier frequency of the incident pulses was set to 1.9 GHz. Fig. 5(a) shows the dispersion curve of the calculated line with the positions of the fundamental and harmonics of the incident carrier waves. Note that the wave number of the 2nd harmonic becomes non-zero. Moreover, the wave number of the 3rd harmonic wave becomes close to that of the fundamental wave. Fig. 5(b) shows the numerically obtained waveforms. The analytically expected pulse width is 2.3 ns. By the collision, envelope pulses too develop. In contrast to Fig. 3(b), the wavelengths of the newly developed pulses are comparable to that of the incident ones. Figs. 6(a) and (b) show the temporal waveforms of the incident and newly developed pulses monitored at the 1000th cell. The newly developed pulse has the spectral peak at 5.6 GHz, being close to the 3rd harmonic of the incident pulses.

To obtain the conditions on what harmonics dominantly develop

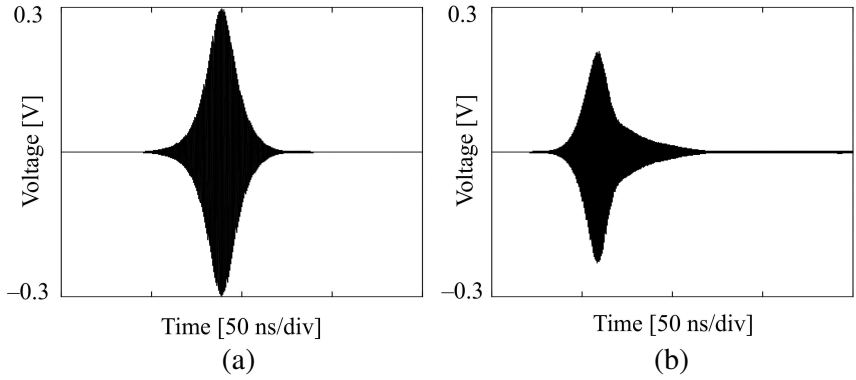

Figure 4. Waveforms of incident and newly developed envelope pulses. The carrier frequency of the incident pulses was 1.6 GHz. The incident and newly developed pulses are shown in Figs. 4(a) and (b), respectively.

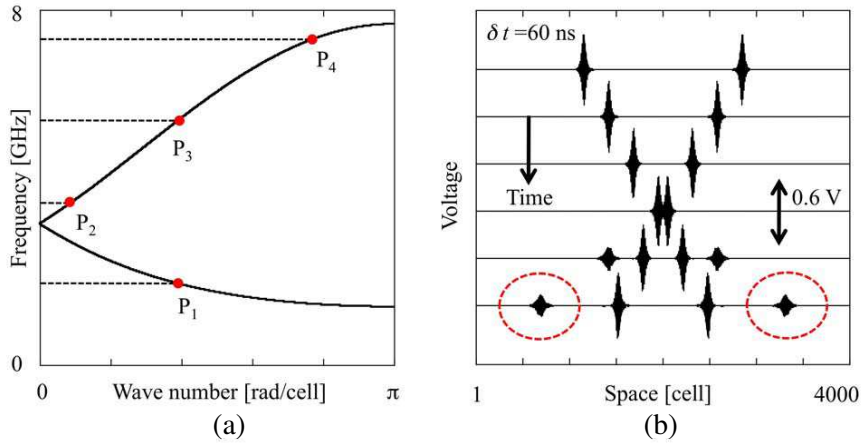

Figure 5. Collision of two nonlinear envelope pulses with 1.9-GHz carrier frequencies. The positions of the fundamental and harmonics on the dispersion curve are shown in Fig. 5(a). The fundamental, 2nd-, 3rd-, and 4th-harmonics are represented by P_1, P_2, P_3, and P_4, respectively. Six spatial waveforms recorded in 60-ns increments are shown in Fig. 5(b). The newly developed pulses are marked with the circles.

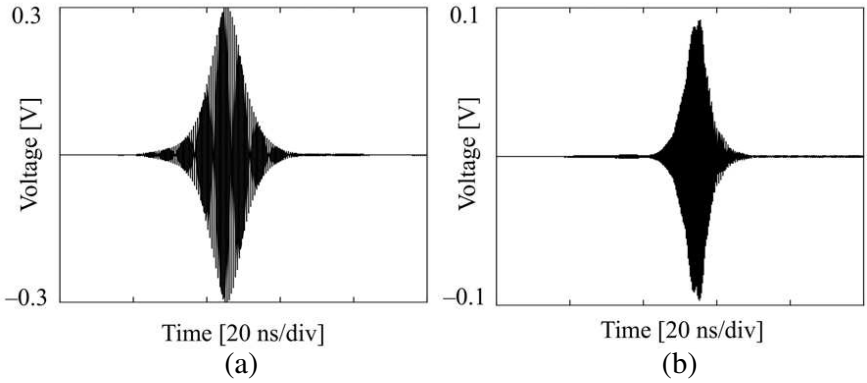

Figure 6. Waveforms of incident and newly developed envelope pulses. The carrier frequency of the incident pulses was 1.9 GHz. The incident and newly developed pulses are shown in Figs. 6(a) and (b), respectively.

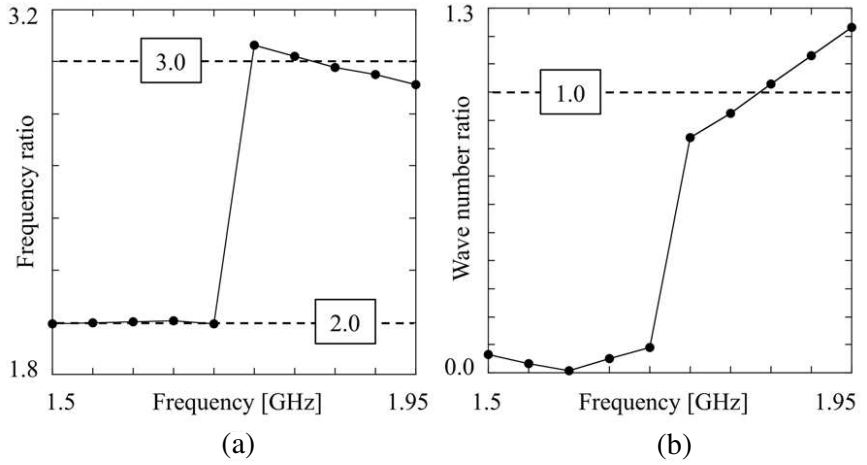

Figure 7. Properties of newly developed envelope pulses. The ratios of (a) the peak frequencies and (b) the peak wave numbers of newly developed pulses to that of incident pulses are shown. Two dashed lines in Fig. 7(a) emphasize the positions where the frequency ratio becomes 2.0 and 3.0. Similarly, the dashed line in Fig. 7(b) emphasizes the position where the wave number ratio becomes 1.0.

by the collision, we carried out similar calculations for several different carrier frequencies. We varied the carrier frequency from 1.5 to 1.95 GHz with the increment of 0.05 GHz. We estimated the frequency corresponding to the spectral peak for both the incident and newly developed pulses. Fig. 7(a) shows the ratio of the peak frequencies of newly developed pulses to that of incident pulses. We can see that the 2nd harmonic dominates the newly developed pulses for carrier frequencies $\leq$ 1.7 GHz, and the 3rd harmonic dominates them for carrier frequencies $\geq$ 1.75 GHz. Similar spectral analysis was done for the spatial waveforms to obtain Fig. 7(b). The ratios of the peak wave number of newly developed pulses to that of incident pulses are shown. Consistently, the ratios of the wave numbers are close to zero for carrier frequencies $\leq$ 1.7 GHz, and are close to unity for carrier frequencies $\geq$ 1.75 GHz.

As is well known [15], the efficiently of the harmonic-wave generation in two-wave mixing becomes maximal, when the phase-matching condition is satisfied, which is given by

$$k_3 \sim m_1 k_1 + m_2 k_2, \tag{4}$$

where k_1 and k_2 represents the wave numbers of incident waves, and k_3 represents that of the newly generated harmonic wave. Moreover, m_1 and m_2 are integers to be specified by the order of generated harmonics. At present, incident pulses have the common carrier frequency, and one travels to the left and the other to the right, resulting in the condition

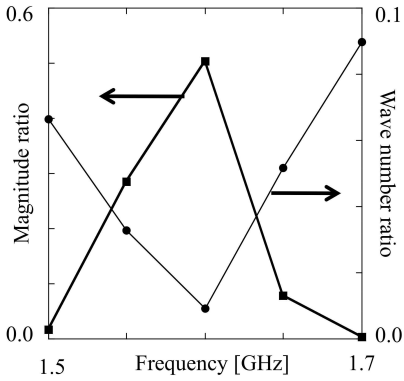

Figure 8. Efficiency of harmonic-wave generation. The left vertical axis indicates the ratio of the spectral magnitude of the newly developed 2nd harmonic frequency and that of the incident fundamental frequency. Moreover, the right vertical axis indicated the ratio of the wave numbers of the newly developed and incident pulses.

$k_1 = -k_2 \equiv k_0$. For the 2nd harmonic generation, both m_1 and m_2 have to be equal to 1. Hence, the maximal 2nd harmonic generation can be observed, when $k_3 \sim 0$. Similarly, for the 3rd harmonic generation, k_3 has to be close to k_0. The numerically obtained result mentioned above can be well explained by what types of the phase-matching dominates the newly developed pulses, when taking CRLH lines' dispersion into consideration. Fig. 8 reinforces this observation. The ratio of the spectral magnitude of the newly developed 2nd harmonic frequency and that of the incident fundamental frequency is shown by the thick curve. It becomes maximal at 1.6 GHz. On the other hand, the thin curve shows the ratio of the wave numbers of the newly developed and incident pulses. We can see that the maximal efficiency of the 2nd harmonic generation is observed when the wave number of newly developed pulses approaches zero mostly. Similar behavior of the 3rd harmonic magnitude is observed for carrier frequencies ≥ 1.75 GHz, although it becomes more complicated than in Fig. 8, because the 4th-harmonic pulses develop at the same time at around 1.85 GHz.

Finally, we examined the influences of losses. As an estimate of the loss magnitude, we considered the typical parasitic resistance of microwave surface-mount inductors, which is roughly 0.1 Ω. Fig. 9 shows how much the magnitude of the 2nd harmonic wave is degraded by the line resistance. We introduced resistors in series to both L_R and L_L, whose resistance was varied from 0.1 to 0.5 Ω with the increment of 0.1 Ω. At present, the cell size was 500. The spectral magnitude of the 2nd harmonic wave monitored at the 100th cell is

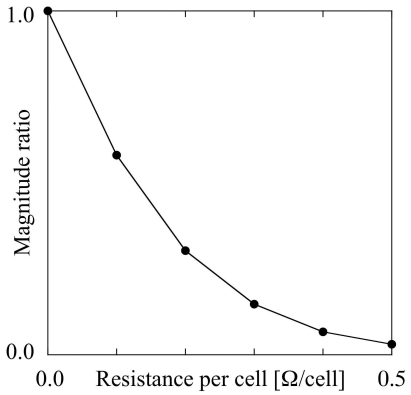

Figure 9. Influence of losses. The normalized magnitude of the newly developed 2nd harmonic wave is shown for five difference values of inductors' parasitic resistance.

shown normalized by the loss-free magnitude. The generation efficiency decreases exponentially. However, the device still has finite efficiency for some practical values of resistances. Optimization of the cell size, the input pulse amplitude and the line parameters will widen its applications.

4. DISCUSSION

As a potential application of colliding nonlinear envelope pulses in Schottky CRLH lines, we consider a leaky-wave antenna for the 2nd-harmonic envelope pulses developed by the collision.

The wave number corresponding to the 2nd harmonic wave, being set close to zero, can be inside the light cone; therefore, some part of the 2nd harmonic pulses may radiate to the direction specified by the wave number.

On the other hand, if the carrier frequency of the right-going pulse f_r is smaller than that of the left-going pulse f_l, the amplitude of the wave vector of the right-going pulse $|k_r|$ becomes larger than that of the left-going one $|k_l|$. As a result, the wave vector of the 2nd harmonic wave directs to the left, because both of incident pulses are carried by the left-handed mode. Then, if the 2nd harmonic wave is carried by the right-handed mode, the newly developed envelope pulse travels to

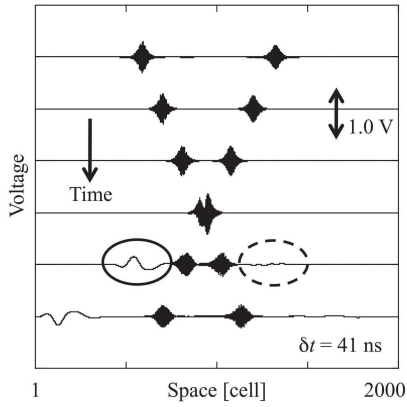

Figure 10. Collision of two nonlinear envelope pulses with incoincident carrier frequencies. The right- and left-going pulses have the carrier frequencies of 1.60 and 1.65 GHz, respectively. The left- and right-going pulses developed by the collision are marked with the solid and dashed circles, respectively.

the left. By the similar consideration, only the right-going envelope pulse develops, if $f_r > f_l$. In Fig. 10, we show the calculated results, where f_r and f_l are 1.60 and 1.65 GHz, respectively. Total cell size was 2000. Six spatial waveforms recorded in 41.0-ns increments are shown. As expected, the left-going pulse dominates the right-going one.

Using these properties, the direction of the radiated pulse can be managed by changing the carrier frequency of one of colliding pulses.

5. CONCLUSION

We characterized the Schottky CRLH line as a platform for interacting nonlinear envelope pulses. Envelope pulses having harmonic carrier frequencies are newly developed by the collision of two nonlinear envelope pulses. The efficiency of the newly developed pulses becomes maximal, when the phase-matching condition is satisfied. The mechanism can potentially be used to manage the directivity of radiating waves as the line operates as a leaky-wave antenna. Although further investigations must be carried out for the methods to develop large pulses, we believe that the line may significantly increase the applications of nonlinear pulses in high-speed electronics.

REFERENCES

1. Hirota, R. and K. Suzuki, "Studies on lattice solitons by using electrical networks," *J. Phys. Soc. Jpn.*, Vol. 28, 1366–1367, 1970.
2. Rodwell, M. J. W., S. T. Allen, R. Y. Yu, M. G. Case, U. Bhattacharya, M. Reddy, E. Carman, M. Kamegawa, Y. Konishi, J. Pusl, and R. Pullela, "Active and nonlinear wave propagation devices in ultrafast electronics and optoelectronics," *Proc. IEEE*, Vol. 82, 1037–1059, 1994.
3. Narahara, K., "Interaction of nonlinear pulses developed in coupled transmission lines regularly spaced Schottky varactors," *Progress In Electromagnetics Research Letters*, Vol. 17, 85–93, 2010.
4. Caloz, C. and T. Itoh, *Electromagnetic Metamaterials: Transmission Line Theory and Microwave Applications*, Wiley, 2006.
5. Monti, G. and L. Tarricone, "Signal reshaping in a transmission line with negative group velocity behaviour," *Microwave Optical Technol. Lett.*, Vol. 51, 2627–2633, 2009.
6. Chi, P. and T. Itoh, "Dispersion engineering with CRLH metamaterials," *Proc. IEEE International Symposium on Radio-Frequency Integration Technology*, 128–131, 2009.

7. Gómez-Diaz, J. S., S. Gupta, A. Álvarez-Melcón, and C. Caloz, "Investigation on the phenomenology of impulse-regime metamaterial transmission lines," *IEEE Trans. Antennas and Propagat.*, Vol. 57, 4010–4014, 2009.
8. Kozyrev, A. B. and D. W. Van Der Weide, "Nonlinear wave propagation phenomena in left-handed transmission-line media," *IEEE Trans. Microwave Theory and Techniques*, Vol. 53, 238–245, 2005.
9. Gupta, S. and C. Caloz, "Dark and bright solitons in left-handed nonlinear transmission line metamaterials," *Proc. of IEEE MTT-S Int. Microwave Symp. 2007*, 979–982, Honolulu, 2007.
10. Kafaratzis, A. and Z. Hu, "Envelope solitons in nonlinear left handed transmission lines," *Proceedings of Metamaterials 2007*, 771–773, 22–24, Rome, 2007.
11. Simion, S., R. Marcelli, G. Bartolucci, G. Sajin, and F. Craciunoiu, "Nonlinear composite right/left-handed transmission line for frequency doubler and short pulse generation," *Proc. of Metamaterials 2008*, 492–494, 2008.
12. Gharakhili, F. G., M. Shahabadi, and M. Hakkak, "Bright and dark soliton generation in a left-handed nonlinear transmission line with series nonlinear capacitors," *Progress In Electromagnetics Research*, Vol. 96, 237–249, 2009.
13. Ogasawara, J. and K. Narahara, "Short envelope pulse propagation in composite right- and left-handed transmission lines with regularly spaced Schottky varactors," *IEICE Electron. Express*, Vol. 6, 1576–1581, 2009.
14. Taniuti, T., "Reductive perturbation method and far fields of wave equations," *Prog. Theor. Phys. Suppl.*, Vol. 55, 1–55, 1974.
15. Boyd, R. W., *Nonlinear Optics*, Academic Press, 2002.